Classical resonances in quantum mechanics

J. Henkel and M. Holthaus*
Physikalisches Institut der Universität Bonn, Nussallee 12, W-5300 Bonn 1, Germany
(Received 15 July 1991)

We study the role of classical resonances in quantum systems subjected to a periodic external force. It is demonstrated that classical invariant vortex tubes determine the structure of Floquet states "captured" by resonances in the classical phase space. In addition, resonance quantum numbers are introduced. The analysis of simple model calculations leads to a qualitative description of nonperturbative phenomena relevant for the interaction of atoms or molecules with strong, short laser pulses.

PACS number(s): 42.50.Hz, 03.65.Sq

I. INTRODUCTION

In recent years, the experimental study of atoms and molecules in strong laser fields has led to the discovery of several exciting and unexpected effects as, for instance, above-threshold ionization [1] and high-harmonic generation [2], which still are not completely understood. In general, these phenomena occur when the laser field is so strong that it cannot be regarded as a small perturbation of the atom. For the theoretician, dealing with strong laser fields is a difficult task, but taking into account the fact that most experiments are performed with short laser *pulses,* the situation appears even more involved: at the initial stage of the pulse, the laser field is "weak," then "strong," and, finally, "weak" again. Also this switching between different regimes of field strength can give rise to essential and systematic effects, some of which we are going to discuss in the present work.

To this end, we will consider periodically time-dependent model systems with a Hamiltonian of the form

$$H^{\lambda}(t)=H_0+\lambda H_{\rm int}(t)\ , \tag{1.1}$$

where H_0 describes the unperturbed atom or molecule and $\lambda H_{\rm int}(t)$ describes the interaction with an external classical laser field of strength λ; of course, λ changes during the pulse.

On the classical level, even simple Hamiltonian systems exhibit chaotic dynamics when subjected to a periodic force; the question whether and how classical chaos manifests itself in the corresponding quantum systems is a subject of intense current research [3]. In this work, we will explore connections between classical and quantum mechanics which are important for strong laser physics; however, we will focus on situations where the classical dynamics is mainly *regular* even for large coupling strength λ.

Zones of predominantly regular motion in the phase space of classical nonintegrable systems are found in "resonances" surrounding elliptic periodic orbits [4]. Generally, the magnitude of such a resonance increases with increasing coupling strength and, if it is large enough, it can support one or more quantum states.

For quantum systems like (1.1) which are periodic in time, the relevant states are the Floquet states [5–8], i.e., the time-periodic eigenstates of the operator

$$\mathcal{H}^{\lambda}=H^{\lambda}-i\partial_t\ , \tag{1.2}$$

with *fixed* coupling strength λ. In a semiclassical approximation, these Floquet states can be obtained by quantizing invariant time-periodic vortex tubes in the extended classical phase space [9]. If the unperturbed classical Hamiltonian H_0 defines an integrable system, the even-dimensional phase space $\{(p,x)\}$ is completely stratified into invariant tori; the set of all trajectories confined to such a torus forms a vortex tube in the extended phase space $\{(p,x,t)\}$ [10]. If we further assume that the system remains integrable under the periodic perturbation $\lambda H_{\rm int}(t)$, the vortex tubes are periodic in time and fill out the total extended phase space. Analogous to the way the invariant tori of integrable autonomous systems can be quantized semiclassically to yield approximately the quantum eigenstates [11], a semiclassical quantization of periodic vortex tubes yields the Floquet states. For a system with N degrees of freedom the quantization rules are

$$\oint_{\gamma_i}(p\,dx-H\,dt)=2\pi\hbar\left[n_i'+\frac{\mathrm{ind}\gamma_i}{4}\right]\ , \qquad i=1,\ldots,N \tag{1.3}$$

$$\varepsilon=-\frac{1}{T}\int_{\gamma_{N+1}}(p\,dx-H\,dt)+\hbar\omega m,\quad m\in\mathbb{Z}\ . \tag{1.4}$$

In these formulas, T denotes the periodicity interval and $\omega=2\pi/T$. The paths γ_i are topologically inequivalent basis cycles of the first homology group of the vortex tubes with Maslov indices $\mathrm{ind}\gamma_i$, whereas the path γ_{N+1} extends along the vortex tubes in the t direction with periodic boundary conditions. Basically, the conditions (1.3) select the correct "quantized" vortex tubes, Eq. (1.4) then yields the quasienergy ε. A detailed derivation and discussion of these quantization conditions can be found in Ref. [9]. The point which actually is of central importance in our context is the fact that, provided the classical phase space is regular, the Floquet states of time-periodic quantum systems are associated with classical

invariant vortex tubes in a manner that is analogous to the association of eigenstates of time-independent systems with invariant classical tori [11]. Of course, in the generic case the system does not remain integrable under the influence of the periodic perturbation, and the vortex tubes no longer fill out the phase space completely. Nevertheless, by the Kolmogorov-Arnold-Moser theorem, "most" of the vortex tubes continue to exist at least for small values of the coupling strength λ, and numerically one finds indications of preserved vortex tubes even for relatively large λ. Our following model calculations will show that an association of Floquet states with vortex tubes is possible also for near-integrable systems.

Returning now to the problem of matter interacting with strong laser pulses, we are thus led to consider the following scenario: If the field strength λ is very low, the classical resonances are too small to contain vortex tubes which fulfill the semiclassical quantization conditions; the Floquet states closely resemble the eigenfunctions of H_0. However, with increasing λ, the main resonances support more and more Floquet states, whose structures are then governed by the quantized vortex tubes surrounding the elliptic periodic orbits. Therefore those Floquet states that are "captured" by resonances have to change their structure quite significantly.

It is this change of structure and its implications for laser pulse experiments that we will now investigate in some detail. In the following two sections we will provide two experimentally accessible examples for the general scenario outlined above. We will first study the instantaneous dynamics at fixed field strength λ and defer the discussion of laser pulses to the concluding fourth section.

II. FIRST EXAMPLE: MOLECULAR VIBRATIONS IN STRONG LASER FIELDS

In this section we consider the classical and quantum mechanics of vibrations of a molecular bond in the presence of a strong laser field. As usual [12–16], we model this situation by a periodically forced Morse oscillator:

$$H^{\lambda}(p,x,t)=H_0(p,x)-\lambda\mu_0 x e^{-x/x^*}\sin\omega t \ , \tag{2.1}$$

where

$$H_0(p,x)=\frac{p^2}{2M}+D\{1-\exp[-\beta(x-x_e)]\}^2 \ . \tag{2.2}$$

The classical and quantum dynamics of a δ-kicked Morse oscillator have also been investigated in detail recently [17,18].

To be definite, we fix the parameters such that the Hamiltonian (2.1) describes the local O–H stretching modes [19] of a H_2O molecule interacting with a classical laser field of frequency ω and strength λ [20]: $M=1728.53$, $D=0.1994$, $\beta=1.189$, $x_e=1.821$, and $\mu_0=1.634$, $x^*=1.134$ (all data are in atomic units).

After a transformation to action-angle variables (I,θ), the unperturbed classical Hamiltonian H_0 can, for bounded motion, be expressed as

$$H_0(I)=\omega_0 I-\frac{\omega_0^2 I^2}{4D} \ , \tag{2.3}$$

with $\omega_0=(2D\beta^2/M)^{1/2}$; hence the angular frequency is

$$\Omega=\frac{\partial H_0}{\partial I}=\omega_0-\frac{\omega_0^2 I}{2D} \ . \tag{2.4}$$

When the Morse oscillator is driven with frequency ω by an external force, a resonance occurs if the winding number

$$\gamma\equiv\frac{\omega}{\Omega} \tag{2.5}$$

takes on a rational value. Of course, those rationals which are fractions of small integers yield the most important resonances; the most prominent of them, therefore, is characterized by $\gamma=1$.

In contrast to the unperturbed system, the periodically driven Morse oscillator (2.1) is classically nonintegrable. Figure 1 shows a Poincaré surface of section for $\omega=0.016\,015$ a.u. and $\lambda=0.05$ a.u. (corresponding to a photon energy of 0.436 eV and an intensity of 8.77×10^{13} W/cm^2). The structures visible in Fig. 1 are determined by the $\gamma=1$ resonance: The two innermost closed curves surround the elliptic fixed point and encircle areas of action equal to $2\pi\hbar(n'+\frac{1}{2})$ for $n'=0$ and 1, respectively; they are sections of vortex tubes obeying the quantization condition (1.3) with the plane $t=T/4$. The curve corresponding to $n'=2$ has dissolved into a chain of higher-order islands, and a further one which approximately corresponds to $n'=3$ already exhibits sharp edges, thus indicating a nearby stochastic layer which is the boundary of the primary resonance. Since the area of this elliptic island of mainly regular motion is roughly $\frac{7}{2}2\pi\hbar$, one expects the resonance to support four Floquet states.

Before investigating the quantum mechanics of the forced Morse oscillator, a clarifying remark seems appropriate: A classical trajectory with an initial value "inside" the resonance remains confined to the resonance for all times, the invariant periodic vortex tubes persist perpetually. In contrast, in quantum mechanics all Floquet

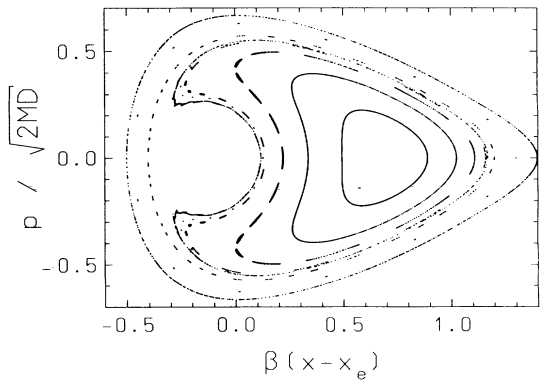

FIG. 1. Poincaré surface of section for the classical driven Morse oscillator (2.1) taken at $t=T/4 \bmod T$. ($\omega=2\pi/T=0.016\,015$ a.u., $\lambda=0.05$ a.u.)

states are decaying. Analogous to the way the tunneling decay in the presence of a static electric field is accounted for by complex energies, the quasienergies are the poles of the resolvent of $\mathcal{H}^{\lambda}=H^{\lambda}-i\partial_t$ in the lower half of the complex quasienergy plane [21]. Hence, because of tunneling effects, in quantum mechanics a *perpetual* localization of probability is impossible.

The calculation of tunneling probabilities obviously is beyond the scope of the simple vortex tube quantization or, more generally, beyond that of a simple series expansion in powers of $\hbar$. On the other hand, for very short laser pulses the tunneling-type decay of the Floquet states can be negligible. To verify that this is actually the case for low Morse eigenstates, we have calculated the final population of bound states and the dissociation probability of the Morse oscillator (2.2) after the ground state has interacted with a short pulse

$$\lambda=\lambda(t)=\lambda_{\max}\sin^2\left[\frac{\pi t}{t_p}\right] \tag{2.6}$$

of length $t_p=0.474$ ps. The results are displayed in Fig. 2 as functions of the peak field strength $\lambda_{\max}$. In this calculation, we have taken the continuum into account explicitly and have employed the same numerical method as in a recent related study [22]. As for the classical surface of section depicted in Fig. 1, the frequency again is $\omega=0.016\,015$. For this frequency, the energy 4ω of four photons is exactly equal to the difference of the energy of the ground state φ_0 and that of the fourth excited state φ_4 of H_0. As can be seen from Fig. 2, the final occupation of these two states alone accounts for most of the probability, whereas the probability of dissociation is less than 10^{-3} even for $\lambda_{\max}=0.10$ a.u. (peak intensity is 3.51×10^{14} W/cm^2). Therefore, in the following quantum calculations we will neglect the tunneling to the continuum altogether and restrict ourselves to the space spanned by the bound states of H_0. In this approximation, the quasienergies are real numbers. Of course,

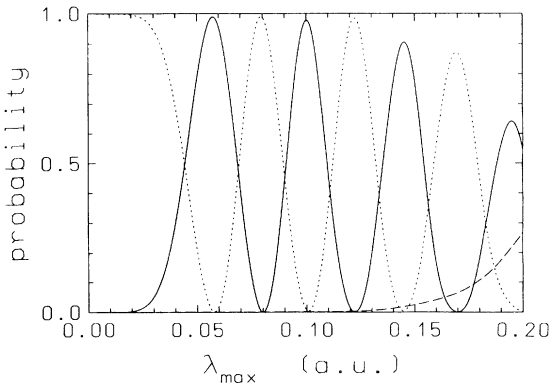

FIG. 2. Occupation probability of the ground state φ_0 (dotted line), of the fourth excited state φ_4 (full line), and dissociation probability (dashes) of the quantum-mechanical Morse oscillator (2.2) after the system has interacted with smooth, short laser pulses with the envelope (2.6). Before the pulses, the system was in its ground state φ_0. ($\omega=0.016\,015$ a.u., $t_p=50\times2\pi/\omega=0.474$ ps.)

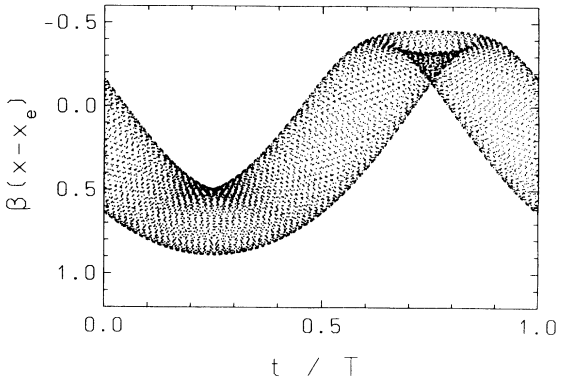

FIG. 3. Projection of the innermost quantized vortex tube ($n'=0$) shown in Fig. 1 to the $\{(x,t)\}$ space.

neglecting the small imaginary parts of the actual quasienergies corresponds to the neglection of the small dissociation probabilities for very short pulses.

After this digression we now turn to the question whether quantized vortex tubes surrounding an elliptic periodic orbit do actually determine the structure of the quantum mechanical Floquet states. Instead of calculating these states for fixed moment t_0 of time and then employing a Husimi coherent-state representation [23], we follow the example of Ref. [9] and compare the full Floquet states $u_\alpha^\lambda(x,t)$ directly with classical objects projected to the $\{(x,t)\}$ configuration space.

As an example, Fig. 3 shows a projection of the innermost quantized vortex tube for the $\gamma=1$ resonance seen in Fig. 1, whereas Fig. 4 exhibits the probability density of the associated Floquet state. Obviously, the occurrence of a relatively high probability density at $t=3T/4$ is connected to a classical "swallow tail" structure. In a similar manner, the Floquet state shown in Fig. 5 is associated with the vortex tube which encloses an area of $2\pi\hbar(1+\frac{1}{2})$ at fixed time (see Fig. 6).

These two examples demonstrate that the spatiotemporal structure of Floquet states can, even for fairly low quantum numbers, strongly be influenced by classical vortex tubes. Of course, not all the Floquet states are associated with resonant vortex tubes in this way. For the

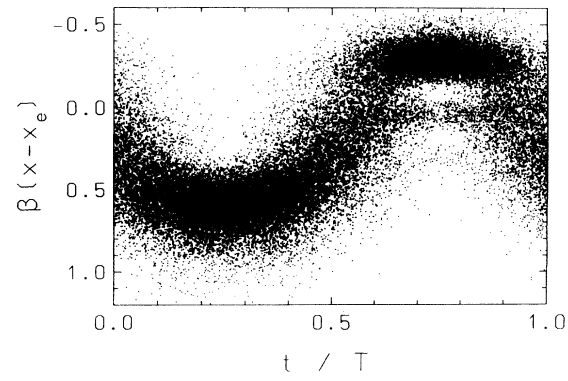

FIG. 4. Probability density $|u^\lambda(x,t)|^2$ of the Floquet state associated with the vortex tube depicted in Fig. 3.

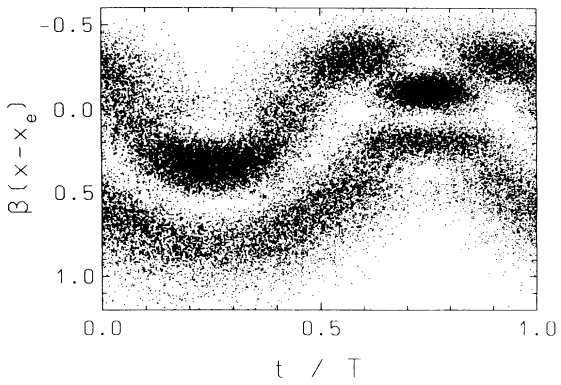

FIG. 5. Probability density $|u^{\lambda}(x,t)|^2$ of the Floquet state associated with the vortex tube depicted in Fig. 6.

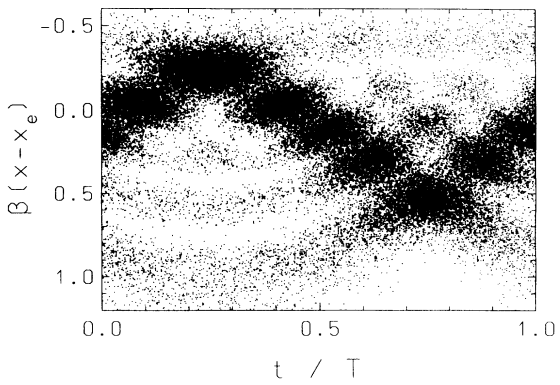

FIG. 8. Floquet state for which the bulk of probability follows the hyperbolic periodic orbit shown in Fig. 7 and oscillates in phase opposition to the laser field.

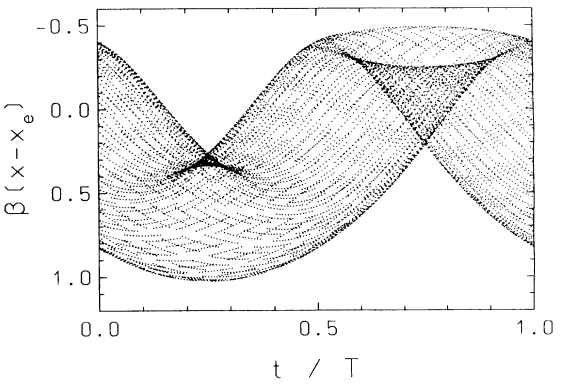

FIG. 6. Projection of the vortex tube with $n'=1$ to the $\{(x,t)\}$ space.

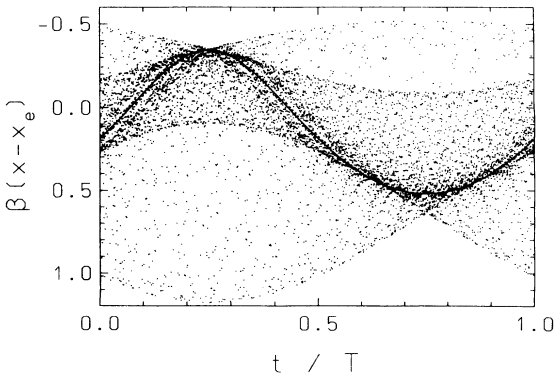

FIG. 7. A hyperbolic periodic orbit for the classical Morse oscillator (2.1) and the trajectory of an orbit with initial conditions in the stochastic layer surrounding the resonance depicted in Fig. 1.

parameters chosen, we find four Floquet states for which this association clearly holds, as expected from the magnitude of the resonance. In addition, other classical phase-space structures also leave their traces in quantum states. For example, in Fig. 7 we exhibit the *hyperbolic* periodic orbit belonging to the resonance in question and, in addition, the trajectory of an orbit with initial value in the thin stochastic layer surrounding the resonance. The probability density of the Floquet state shown in Fig. 8 clearly follows the hyperbolic orbit: an indication of "scarring" [24] in a state with low quantum number. It is remarkable that for this state the bulk of the probability oscillates in phase opposition to the laser field.

A Floquet state associated with a quantized vortex tube is labeled by the quantum number n' which occurs in the semiclassical quantization rules (1.3). This integer n' characterizes the nodal structure of the Floquet state. It is important to note that this "resonance quantum number" n' is, in general, different from the quantum number n the very same Floquet state would carry if all states were labeled by H_0 quantum numbers at $\lambda=0$ and

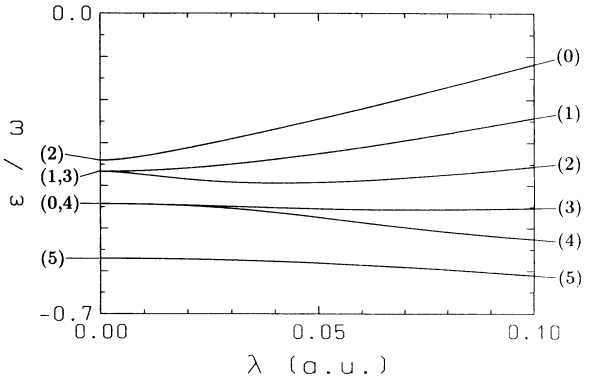

FIG. 9. Part of the quasienergy spectrum (quasienergies ε in units of ω) for the periodically driven Morse oscillator (2.1), $\omega=0.016015$ a.u. Integers on the left margin are H_0 quantum numbers n, integers on the right are resonance quantum numbers n'. At $\lambda=0$, the energies of the states $n=0$ and 4 and, moreover, those of $n=1$ and 3 are exactly degenerate mod ω.

if this assignment of quantum numbers were continuously extended to nonvanishing field strength. This renumbering reflects the restructuring of states captured by classical resonances.

The reorganizing effect of a classical resonance is also quite evident in the quasienergy spectrum: Figure 9 shows some of the quasienergies of the Morse oscillator (2.1) as functions of the field strength λ, labeled by both the H_0 quantum numbers n and the resonance quantum numbers n'. The quasienergies at $\lambda=0$ are given by the energy eigenvalues of H_0 modulo ω and are, therefore, not arranged in any successive order with respect to n in the Brillouin zone. However, after a certain transition regime, the quasienergies of states associated with resonant vortex tubes have organized themselves such that they are nearly equidistant and actually ordered with respect to n' in the strong-field regime.

This fact underlines the ordering influence of a classical resonance and, at the same time, provides a further motivation for the introduction of resonance quantum numbers. In a sense, the reordering of the quasienergy spectrum of quantum systems in strong oscillating fields is analogous to the transition from the Zeemann effect to the Paschen-Back effect found for atoms in static magnetic fields.

III. SECOND EXAMPLE: RYDBERG ATOMS IN STRONG MICROWAVE FIELDS

The parameters of experimentally accessible microwave fields are, of course, very different from those of laser fields. On the other hand, a microwave amplitude of only a few volts per centimeter is comparable to the binding field exerted on a highly excited electron in a Rydberg atom; in this sense, even microwave fields can be "strong." Rydberg atoms in microwave fields [25–28], therefore, are promising candidates for an experimental study of strong field dynamics.

In this section, we will apply the concept of vortex-tube quantization and resonance quantum numbers to a highly excited hydrogen atom interacting with a microwave field. This system has been studied with great effort both experimentally [25,29] and theoretically [30–33] in recent years. A model that has been found to yield even quantitative agreement with experimental data is that of a forced "one-dimensional Hydrogen atom":

$$H^{\lambda}=H_0-\lambda x \sin\omega t \ , \tag{3.1}$$

with

$$H_0=\frac{p^2}{2}+\begin{cases} -\frac{1}{x}, & x>0 \\ \infty, & x\le 0 \end{cases} \ . \tag{3.2}$$

In this case, the winding number γ equals the "scaled frequency" $I^3\omega$, where I is the action variable of the unperturbed classical Hamiltonian.

Let us choose $\omega=2.736\times10^{-6}$ a.u. ($\omega/2\pi=18.00$ GHz) and $\lambda=9.724\times10^{-10}$ a.u. (5.0 V/cm). Figure 10 then shows a Poincaré surface of section for the classical system, taken at $t=T/4 \bmod T$ ($T=2\pi/\omega$). We observe the primary resonance island surrounded by a zone of connected stochasticity, the closed curves inside this island again encircle areas of $2\pi\hbar(n'+\frac{1}{2})$.

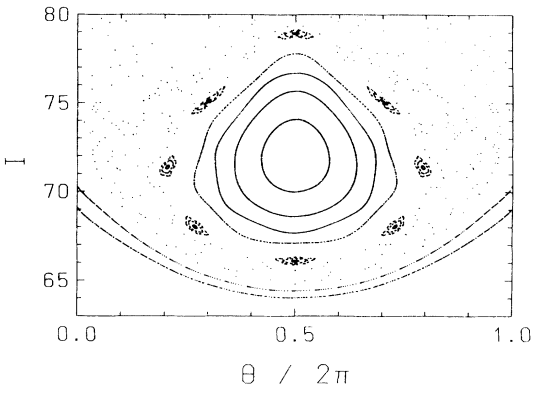

FIG. 10. Poincarè surface of section for the model (3.1) taken at $t=T/4 \bmod T$. ($\omega=2.736\times10^{-6}$ a.u., $\lambda=9.724\times10^{-10}$ a.u.) I and θ are the action-angle variables of the unperturbed system (3.2).

Figure 11 shows a projection of the innermost quantized vortex tube, whereas Fig. 12 shows the obviously associated Floquet wave function. It is noteworthy that this state with resonance quantum number $n'=0$ develops continuously from the H_0 eigenfunction with $n=72$ when the field strength λ is increased.

Figures 13–15 show the Floquet states with resonance quantum numbers $n'=1$, 2, and 3. These figures demonstrate in a striking manner that it is the resonance quantum number which contains the essential information about the Floquet states. It is only consequent to regard the state with $n'=0$ (Fig. 12) not as an excited state of the Hydrogen atom but rather as the ground state of an object with a size of about 10 000 a.u. Correspondingly, the states with $n'>0$ are the excited states of this object.

The following table shows which H_0 eigenstates are deformed into which resonance eigenstates in the present example:

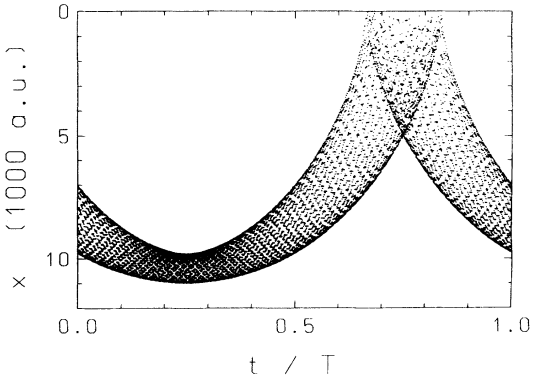

FIG. 11. Projection of the innermost quantized vortex tube seen in Fig. 10 to the $\{(x,t)\}$ space.

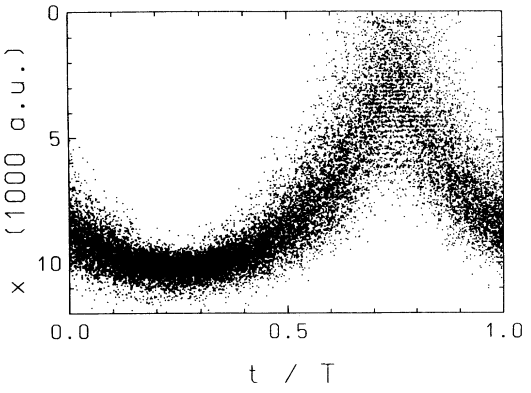

FIG. 12. Probability density of a Floquet state with $n'=0$ associated with the vortex tube depicted in Fig. 11.

n'	n
0	72
1	71
2	73
3	70
4	74
5	69

As it has been found for the driven Morse oscillator, the ordering influence of the classical resonance reflects itself also in the quasienergy spectrum (Fig. 16). Again, in the strong field regime the quasienergies are successively ordered with respect to the resonance quantum number n'. The characteristic treelike appearance of the quasienergies of near-resonant states does not depend on the special choice of the parameters; it has also been found in other spectra [34,35]. It is interesting to note that the effect of the resonance on the spectrum is even greater than expected: The island shown in Fig. 10 contains only four quantized vortex tubes, but the quasienergy spectrum shows several more states which clearly follow the systematic reordering of the near-resonant levels.

As a technical side remark we would like to point out

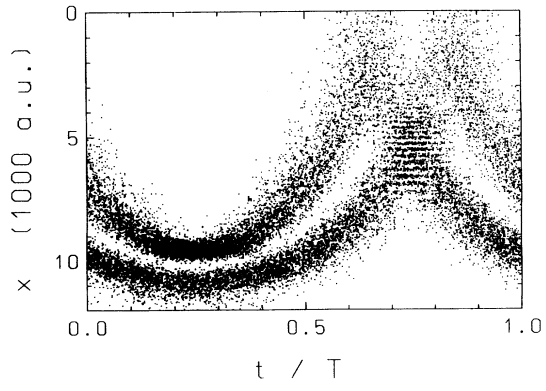

FIG. 13. Probability density of a Floquet state with $n'=1$.

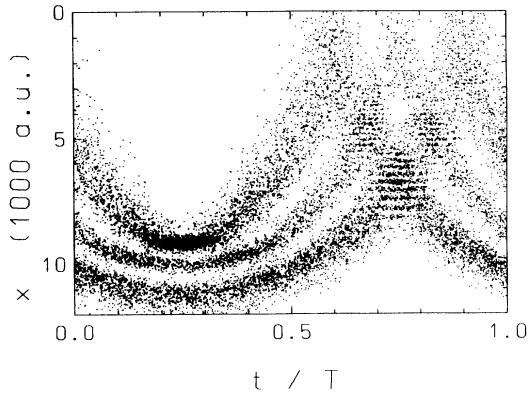

FIG. 14. Probability density of a Floquet state with $n'=2$.

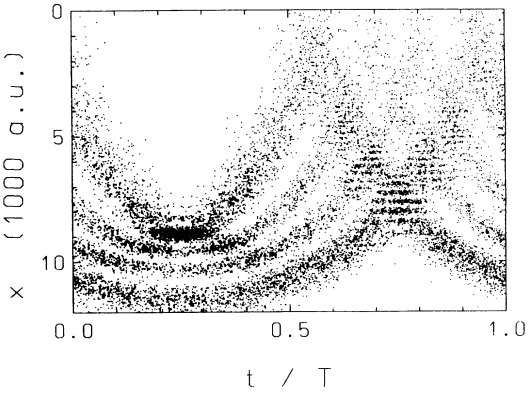

FIG. 15. Probability density of a Floquet state with $n'=3$.

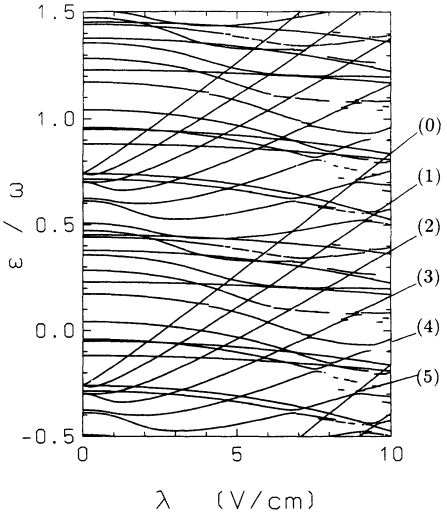

FIG. 16. Two Brillouin zones of quasienergies for the model (3.1) and $\omega=2.736\times10^{-6}$ a.u. Near-resonant states are labeled by resonance quantum numbers n' (right margin). The quasienergies shown develop from the energies of the eigenstates with $n=60-80$ of the unperturbed system (3.2).

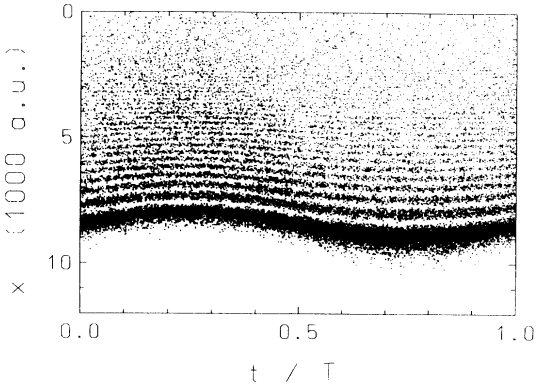

FIG. 17. Probability density of a Floquet state which still closely resembles an eigenfunction of the unperturbed system (3.2). The parameters are the same as in Fig. 10.

that it is advantageous to investigate the structure of the full Floquet states instead of considering merely the eigenstates of the "one-cycle-evolution operator" [31,36] that strongly depend on the phase of the external field (see also the discussion in Ref. [33]). For example, a section of the state with $n'=0$ (see Fig. 12) taken at $t=3T/4$ hardly reveals the essential features; furthermore, such a section of the same state would appear completely different when taken at $t=T/4$. The strategy of calculating the full Floquet states removes this arbitrariness. It is also useful for the investigation of states which are not dominated by a classical resonance: Figure 17 shows a Floquet state with $n=66$, which, at $\lambda=5$ V/cm, still closely resembles the H_0 eigenfunction, whereas Fig. 18 shows a Floquet state in the transition regime. Also in this case, looking at the state merely at $t=3T/4$ might be misleading because the concentration of probability at this particular instant of time is not found at other moments.

IV. DISCUSSION AND CONCLUSIONS

In the two examples studied in the preceding sections, the field strength λ differs by more than seven orders of magnitude. Nevertheless, these examples share a common physical ground: In both cases, resonances in the classical phase space provide a key for understanding quantum mechanics in the strong field regime. Classical vortex tubes surrounding elliptic periodic orbits determine the structure of near-resonant instantaneous Floquet states $u_\alpha^\lambda(x,t)$ which, in turn, are no longer characterized by the quantum numbers of the unperturbed system but by the new resonance quantum numbers instead. In addition, the first example shows that the association of classical vortex tubes with Floquet states, although being a semiclassical concept [9], may also hold for very low quantum numbers.

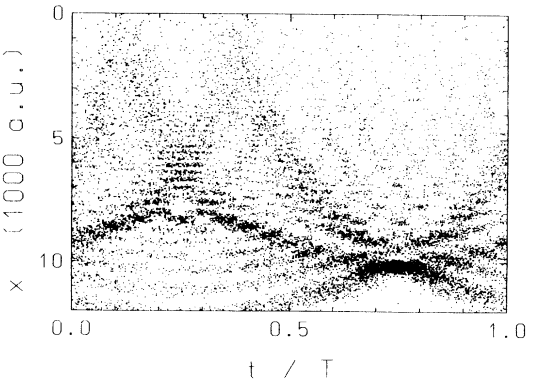

FIG. 18. Probability density of a Floquet state in the transition region; parameters are the same as in Fig. 10.

But in the case of short laser pulses we are not primarily interested in the structure of instantaneous Floquet states for a fixed field strength λ, but rather in the solutions of the time-dependent Schrödinger equation

$$i\partial_t\psi(t)=[H_0+\lambda(t)H_{\rm int}(t)]\psi(t)\ . \tag{4.1}$$

It is one of the major advantages of the Floquet picture that it also allows for the investigation of this problem. What connects a "static" analysis performed in terms of instantaneous Floquet states with the dynamical problem of laser pulses is the fact that the Floquet states respond adiabatically to a variation of the field strength: If the laser amplitude changes sufficiently slowly, the initial state is shifted into the connected Floquet state [37]. But what "sufficiently slowly" actually means in a given situation depends strongly on details. In our examples, the instantaneous Floquet states are deformed from H_0 eigenstates for vanishing λ to resonance eigenstates at large field strength. Correspondingly, in these cases the characteristic pulse length t_p which still allows for approximately adiabatic evolution is considerably longer than for nonresonant initial conditions where no such change of structure is met. If, on the other hand, the pulse length is shorter than this characteristic time, the wave function $\psi(t)$ can no longer follow the instantaneous Floquet states adiabatically, but evolves into a superposition of several of them. This is exactly the physics that underlies the numerical result depicted in Fig. 2: The pulse length of $t_p=474$ fs amounts to only 50 optical cycles, an interval which is too short for the wave function to follow the resonance-induced change of structure of the instantaneous Floquet states. Instead, it splits into a superposition of those two Floquet states that develop from the initially resonant vibrational states. On the other hand, t_p is still long enough to enable approximately adiabatic evolution of these two coupled states. Even for pulses with a peak field strength of $\lambda_{\rm max}=0.1$ a.u., almost all the probability remains in the effective space spanned by the two Floquet states at each moment of time. The occupation of final states after the pulses is mainly determined by the fact that both components of the "split" wave function interact again at the end of the pulse and interfere. The conspicuous excitation function of the fourth excited state seen in Fig. 2, therefore, actually is an interference pattern [22,38].

Summarizing, from the Floquet point of view experiments performed with near-resonant, short, strong laser

pulses appear as "deformation and restructuring" experiments: When the field strength increases during the pulse, the instantaneous Floquet states are continuously deformed such that they acquire the vortex tube-dominated resonance structure. But for very short pulses, the wave function cannot follow this strong change of structure adiabatically, but rather splits into a superposition of several Floquet states, which then may interfere at later stages of the pulse and thereby determine the final-state population.

Our first example of molecular bonds in strong laser fields sheds some light on the problem of selective excitation of molecular vibrational states by ultrashort laser pulses [20,39]. This topic is of fundamental importance in laser-assisted chemistry: The possibility of selectively exciting a definite vibrational state on time scales shorter than that characteristic for intramolecular vibrational-energy redistribution opens new ways of systematically controlling a chemical reaction [40]. The interpretation of Fig. 2 indicates a possible physical mechanism [22,38]: If the laser frequency is chosen such that the initial state splits into a superposition of two Floquet states and if the laser pulse is shaped such that it leads to a constructive interference of these two states, an almost complete, selective excitation of vibrational states is possible even in the subpicosecond time domain. The present classical considerations provide a further piece of information to understand this quantum-mechanical phenomenon: The splitting of the wave function is made possible by the resonance-induced change of structure of the instantaneous Floquet states. Correspondingly, in order to achieve a high degree of excitation the laser frequency should be chosen such that initial and target state are classically coupled by a resonance with winding number $\gamma=1$. A more detailed discussion of the classical mechanics relevant for selective excitation will be given elsewhere.

Our second example is of interest for the interpretation of experimental results obtained with highly excited hydrogen atoms. It has been observed that initial hydrogenic states corresponding to resonant values of the "scaled frequency" (i.e., the winding number) are relatively difficult to ionize [41]. It was then pointed out by Jensen [36] that in classical mechanics resonances act stabilizing, but a quantum-mechanical explanation was supposed to be difficult because of possible multiphoton transitions of all orders [33]. But taking into account that Floquet states are associated with quantized vortex tubes inside elliptic islands of regular motion, the problem does not appear that complicated. The Floquet states associated with the innermost quantized tubes, i.e., those states with the lowest resonance quantum numbers, have to tunnel the largest distance in phase space until ionization is possible. Therefore we expect a hierarchy of stability of Floquet states that is determined by the resonance quantum number. This expectation is related to an observation that can be made in the quasienergy spectra: The lower the resonance quantum number, that is, the better the Floquet states inside an island of regular motion are "screened" from the surrounding zone of stochasticity, the higher the field strength at which relevant avoided crossings appear, which enable transitions to other Floquet states [34,35].

An experimental verification of the prediction of a hierarchical order of lifetimes of Floquet states captured by classical resonances obviously requires a careful preparation of individual Floquet states. In principle, this can be achieved by a slow turn-on of the microwave field, so slow that the wave function has time enough to follow the structural change of the instantaneous Floquet states without "splitting." This way of selectively populating individual Floquet states should not be described in terms of multiphoton transitions, it is rather a matter of continuous deformation. The time scale necessary to guarantee an adiabatic turn-on for near-resonant states can be longer than that used in present experiments [34]. It would, therefore, be of interest to measure the ionization probabilities of near-resonant initial Rydberg states as functions of the turn-on time. For an approximately adiabatic turn-on of the microwave field, the order of stability as expressed by the resonance quantum numbers should show up. In any case, the relative stability that has already been observed at resonant values of the scaled frequency appears to indicate another example of "orderly microwave ionization" [42].

As a final conclusion, we suggest to exploit the physical similarity of the two systems we have considered to illustrate the role of classical resonances in laser physics. Selectively exciting a definite molecular vibrational state would be a big step forward in laser-assisted chemistry [40], but this goal may be difficult to achieve at present because it requires accurately shaped laser pulses. On the other hand, in microwave experiments the pulse shape can be controlled with high precision [29]. The resonance-induced change of structure that makes possible the selective excitation of molecular vibrational states can also be found in the case of highly excited hydrogen atoms interacting with a microwave field. It seems, therefore, tempting to model excitation processes that are relevant for molecular physics in experiments with Rydberg atoms exposed to pulsed microwave fields. In view of the importance that selective excitation has for modern chemistry and to stimulate further research, such an enterprise should be worth the effort.

ACKNOWLEDGMENTS

It is a pleasure to thank Professor Dr. K. Dietz for discussions and support. We have also benefitted from discussions with Dr. H. P. Breuer and Professor Dr. J. Manz. We thank the staff of the Regionales Hochschulrechenzentrum der Universität Bonn for making possible extensive use of their FPS 500 computer. This work was supported in part by the Deutsche Forschungsgemeinschaft (Schwerpunktprogramm Atom- und Molekültheorie).

*Present address: Department of Physics, Center for Nonlinear Science, University of California, Santa Barbara, CA 93106.

[1] R. R. Freeman and P. H. Bucksbaum, J. Phys. B **24**, 325 (1991).
[2] M. Ferray, A. L'Huillier, X. F. Li, L. A. Lompré, G. Mainfray, and C. Manus, J. Phys. B **21**, L31 (1988).
[3] See, e.g., *Quantum Chaos,* edited by H. A. Cerdeira, R. Ramaswamy, M. C. Gutzwiller, and G. Casati (World Scientific, Singapore, 1991).
[4] A. J. Lichtenberg and M. A. Lieberman, *Regular and Stochastic Motion* (Springer, New York, 1983).
[5] J. H. Shirley, Phys. Rev. **138**, B979 (1965).
[6] Ya. B. Zel'dovich, Zh. Eksp. Teor. Fiz. **51**, 1492 (1966) [Sov. Phys. JETP **24**, 1006 (1967)].
[7] V. I. Ritus, Zh. Eksp. Teor. Fiz. **51**, 1544 (1966) [Sov. Phys. JETP **24**, 1041 (1967)].
[8] For a recent review, see S. I. Chu, Adv. Chem. Phys. (to be published).
[9] H. P. Breuer and M. Holthaus, Ann. Phys. (N.Y.) **211**, 249 (1991).
[10] V. I. Arnold, *Mathematical Methods of Classical Mechanics* (Springer, New York, 1978).
[11] V. P. Maslov and M. V. Fedoriuk, *Semi-classical Approximation in Quantum Mechanics* (Reidel, Dordrecht, 1981).
[12] R. B. Walker and R. K. Preston, J. Chem. Phys. **67**, 2017 (1977).
[13] Y. Gu and J. M. Yuan, Phys. Rev. A **36**, 3788 (1987).
[14] M. E. Goggin and P. W. Milonni, Phys. Rev. A **37**, 796 (1988).
[15] J. J. Tanner and M. M. Maricq, Phys. Rev. A **40**, 4054 (1989).
[16] R. Graham and M. Höhnerbach, Phys. Rev. A **43**, 3966 (1991).
[17] J. Heagy and J. M. Yuan, Phys. Rev. A **41**, 571 (1990).
[18] Z. M. Lu, J. F. Heagy, M. Vallières, and J. M. Yuan, Phys. Rev. A **43**, 1118 (1991).
[19] J. S. Wright and D. J. Donaldson, Chem. Phys. **94**, 15 (1985).
[20] W. Jakubetz, B. Just, J. Manz, and H. J. Schreier, J. Phys. Chem. **94**, 2294 (1990); B. Just, Diploma thesis, Universität Würzburg, 1991.
[21] K. Yajima, Commun. Math. Phys. **87**, 331 (1982).
[22] H. P. Breuer, K. Dietz, and M. Holthaus, Phys. Rev. A **45**, 550 (1991).
[23] G. Radons and R. E. Prange, Phys. Rev. Lett. **61**, 1691 (1988).
[24] E. J. Heller, Phys. Rev. Lett. **53**, 1515 (1984).
[25] J. E. Bayfield and P. M. Koch, Phys. Rev. Lett. **33**, 258 (1974).
[26] R. C. Stoneman, D. S. Thomson, and T. F. Gallagher, Phys. Rev. A **37**, 1527 (1988).
[27] R. Blümel, R. Graham, L. Sirko, U. Smilansky, H. Walther, and K. Yamada, Phys. Rev. Lett. **62**, 341 (1989).
[28] W. van de Water, S. Yoakum, T. van Leeuwen, B. E. Sauer, L. Moorman, E. J. Galvez, D. R. Mariani, and P. M. Koch, Phys. Rev. A **42**, 572 (1990).
[29] P. M. Koch, L. Moorman and B. E. Sauer, Comments At. Mol. Phys. **25**, 165 (1990).
[30] J. G. Leopold and I. C. Percival, J. Phys. B **12**, 709 (1979).
[31] R. Blümel and U. Smilansky, Z. Phys. D **6**, 83 (1987).
[32] G. Casati, B. V. Chirikov, D. L. Shepelyansky, and I. Guarneri, Phys. Rep. **154**, 77 (1987).
[33] R. V. Jensen, S. M. Susskind, and M. M. Sanders, Phys. Rep. **201**, 1 (1991).
[34] H. P. Breuer, K. Dietz, and M. Holthaus, Z. Phys. D **18**, 239 (1991).
[35] H. P. Breuer and M. Holthaus, J. Phys. (Paris) II **1**, 437 (1991).
[36] R. V. Jensen, Phys. Scr. **35**, 668 (1987).
[37] H. P. Breuer, K. Dietz, and M. Holthaus, in *Coherent Radiation Processes in Strong Fields,* edited by V. L. Jacobs (Gordon and Breach, New York, in press).
[38] H. P. Breuer, K. Dietz, and M. Holthaus, J. Phys. B **24**, 1343 (1991).
[39] G. K. Paramonov and V. A. Savva, Phys. Lett. **97A**, 340 (1983).
[40] J. E. Combariza, C. Daniel, B. Just, E. Kades, E. Kolba, J. Manz, W. Malisch, G. K. Paramonov, and B. Warmuth, in *Isotope Effects in Chemical Reactions and Photodissociation Processes,* edited by J. A. Kaye, ACS Symposium Series (American Chemical Society, Washington, DC, in press).
[41] K. A. H. van Leeuwen, G. v. Oppen, S. Renwick, J. B. Bowlin, P. M. Koch, R. V. Jensen, O. Rath, D. Richards, and J. G. Leopold, Phys. Rev. Lett **55**, 2231 (1985).
[42] T. F. Gallagher, Comments At. Mol. Phys. **25**, 159 (1990).

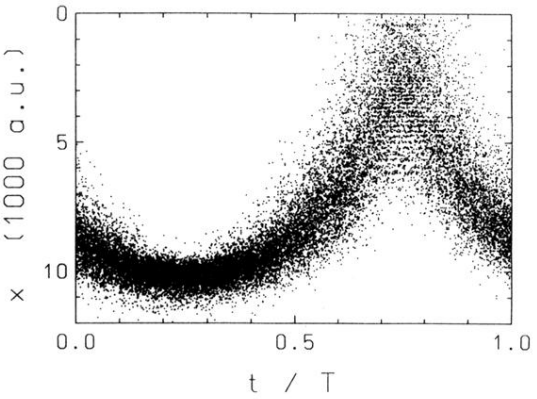

FIG. 12. Probability density of a Floquet state with $n'=0$ associated with the vortex tube depicted in Fig. 11.

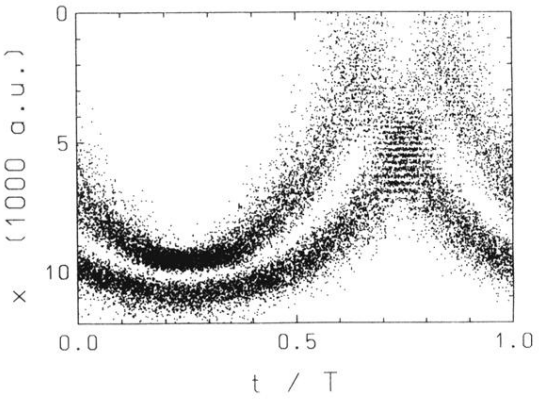

FIG. 13. Probability density of a Floquet state with $n' = 1$.

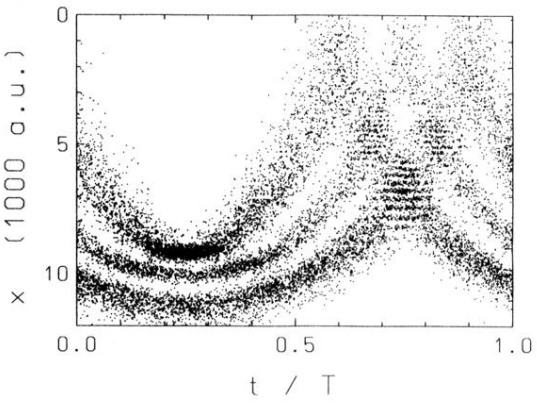

FIG. 14. Probability density of a Floquet state with $n'=2$.

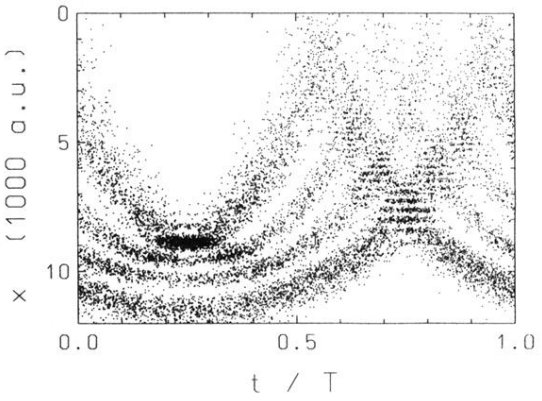

FIG. 15. Probability density of a Floquet state with $n'=3$.

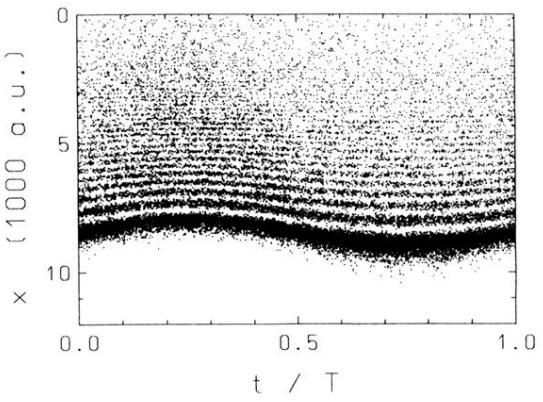

FIG. 17. Probability density of a Floquet state which still closely resembles an eigenfunction of the unperturbed system (3.2). The parameters are the same as in Fig. 10.

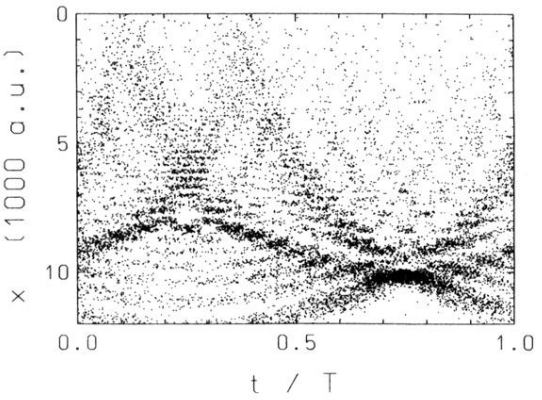

FIG. 18. Probability density of a Floquet state in the transition region; parameters are the same as in Fig. 10.

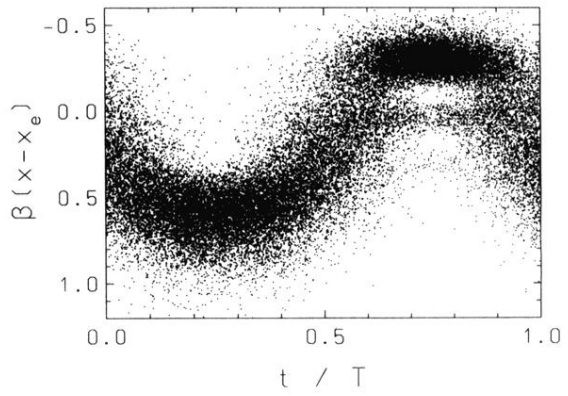

FIG. 4. Probability density $|u^{\lambda}(x,t)|^2$ of the Floquet state associated with the vortex tube depicted in Fig. 3.

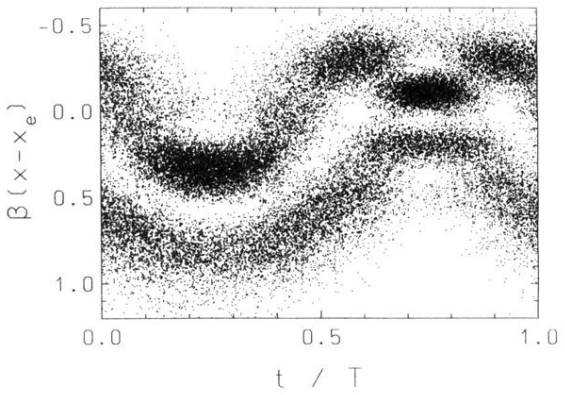

FIG. 5. Probability density $|u^{\lambda}(x,t)|^2$ of the Floquet state associated with the vortex tube depicted in Fig. 6.

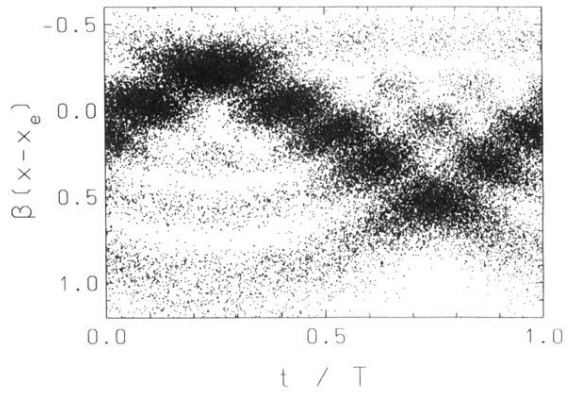

FIG. 8. Floquet state for which the bulk of probability follows the hyperbolic periodic orbit shown in Fig. 7 and oscillates in phase opposition to the laser field.